Title: Development and Characterisation of iron millscale particles reinforced ceramic matrix composite

Author: Stephen I. Durowaye Olatunde I. Sekunowo
Abdulganiyu I. Lawal Olusola E. Ojo

PII: S1658-3655(16)30058-9
DOI: http://dx.doi.org/doi:10.1016/j.jtusci.2016.08.005
Reference: JTUSCI 325

To appear in:

Received date: 27-6-2016
Revised date: 25-8-2016
Accepted date: 29-8-2016

Please cite this article as: S.I. Durowaye, O.I. Sekunowo, A.I. Lawal, O.E. Ojo, Development and Characterisation of iron millscale particles reinforced ceramic matrix composite, *Journal of Taibah University for Science* (2016), http://dx.doi.org/10.1016/j.jtusci.2016.08.005

Development and Characterisation of iron millscale particles reinforced ceramic matrix composite

Stephen I. Durowaye [a,] , Olatunde I. Sekunowo [a], Abdulganiyu I. Lawal [a], Olusola E. Ojo [b]

[a] *Department of Metallurgical and Materials Engineering, University of Lagos, Akoka, Lagos, Nigeria*
[b] *Federal Institute of Industrial Research (FIIRO), Oshodi, Lagos, Nigeria*

** Corresponding author. Tel.: +234 8036844029.*
E-mail address: durosteve02@yahoo.com (S.I. Durowaye).

Abstract

The quest for quality brake pads used by aircrafts and automobiles to ensure effectiveness and safety continues to attract attention. Hence, this study was carried out as part of global efforts at tackling the problem of low durability of these friction materials. Iron millscale (IMS) particles reinforced ceramic matrix composite (CMC) was developed by powder metallurgy method and characterised. The IMS particles addition varied from 5 – 30 wt. % in each CMC produced at different particles size distribution (106- 250 µm) using silica (SiO_2), magnesia (MgO), and sodium bentonite as matrices. On the basis of close correlation between structure and property, the CMCs were subjected to physical, mechanical, and microstructural characterisation using X-ray Fluorescence (XRF), X-ray Diffraction (XRD,) and Scanning Electron Microscopy with Energy Dispersive Spectroscopy (SEM/EDS). The composite exhibits desirable physical and mechanical properties in terms of density (2.97 g/cm^3), porosity (1.24 %), linear shrinkage (1.39 %), impact energy (43.07 J), and compressive strength (114.17 MN/m^2). These values compare very well with the values of brake pads obtained in previous works and conventional/commercial brake pads indicating a potential for effective performance in service.

Keywords: Iron millscale; Ceramic composite; Characterisation; Brake pads

1. Introduction

In an attempt to effect significant improvement in the functional characteristics of brake pads of aircrafts and automobiles, different materials have been used and this has resulted into the development of different types of brake pads [1-4]. However, these brake pads are still known to be plagued by performance related issues such as wear, thermal instability, warpage and low durability [5]. The quest for quality brake pads cannot be divorced from the development of appropriate advanced materials with superlative characteristics [6]. This explains the reason why friction materials that are used in brake pad components are usually heterogeneous. They are meant to demonstrate improved wear resistance at low and high temperatures, rigidity, durability, and make less noise. Thus, during production, formulations are made by varying the weight percentages of the constituent materials in a manner that gives rise to an effective modification in the structure, physical and mechanical properties of the brake pad component [1].

The physical characterisation of a material is one of the scientific techniques

that is normally employed to investigate its intrinsic properties' potential areas of application. The technique is also often used to isolate potent elements/compounds in a material for optimum utilisation. Such discovery is meant to guide the appropriate processing method to which the material is amendable and that will best induce its desirable characteristics. Thus, preliminary subjection of materials to relevant physical characterisation using appropriate technology is imperative. This is more germane when such materials are being considered for advanced applications.

Ceramic matrix composites dispersed with metallic particles are one of the promising materials for high performance applications under severe environment such as high temperature [7]. These materials offer the possibility of combining heat resistance, degradation resistance, and wear resistance due to the ceramic phase with mechanical strength and thermal conductivity provided by the metallic phase [8]. Thus ceramic metal composites (CMCs) are nowadays the candidates for functionally graded materials developed for their multiple functions at reduced cost [9]. They are used as functional components in brake assembly, jet fighters, furnace materials, energy conversion systems, gas turbines, heat engines, etc.

This paper focuses on the development, physical, and microstructural characterisation of iron millscale reinforced hybrid ceramic composite with a view of determining its suitability for aircraft brake pad application.

2. Methodology

2.1. Materials

The reinforcement material used in this study is iron millscale particles while the hybrid matrices are silica sand, magnesia, and bentonite clay. Iron millscale particles were sourced from Universal Steel Nigeria Limited located in Ogba, Lagos. Silica sand was obtained from the beach of the Lagos Atlantic Ocean (bar beach). Magnesia and bentonite clay powders were obtained from a local vendor within the chemicals supplier trade group registered in Nigeria but were manufactured in China and Wyoming, USA respectively.

2.2. Materials characterisation

The elemental composition and phases present in the materials were determined using an X-ray Fluorescence (XRF) spectrometer (model, ARL9400XP+ Thermo, Switzerland) and an X-ray Diffractometer (model GBC Enhanced Material Analyser, Australia) respectively.

2.3. Hybrid ceramic composites production

2.3.1. Materials milling and blending

Iron millscale was milled using a steel ball mill (model A50 43, Mashine, France) and sieved to particles size distribution 106-250 µm using standardised sieves (BSS). The matrix containing 212 µm silica sand, 53 µm magnesia, and 15 µm bentonite was separately mixed with the iron millscale and clean water amounting to 12 wt. % of the total mixture was added. By manual mixing, a uniform distribution of reinforcement particles in the matrix blend was achieved and 80 g the wet blended materials were fed into metallic moulds (Table 1).

2.3.2. Compaction

The Green samples were obtained by uniaxial cold pressing (330 KN/m^2) using a hydraulic press (Capacity 100T, Type P100 EH, Model No. 38280, Weber Hydraulik, Germany) to enhance surface smoothness of the samples. Little lubricant was rubbed on the inner part of the moulds as a releasing agent for easy discharge of the samples from the moulds after compaction.

2.3.3. Drying and sintering

The samples were dried in open air for 3 days, followed by drying under a controlled humidity using an oven dryer at 110^0 C for 24 hours to expel any moisture left in the composite and to avoid cracking during sintering. In order to facilitate the bonding of powder particles (vitrification), the compacted samples were gradually heated to temperatures below the melting point of the materials but high enough to develop significant solid state diffusion. Sintering was carried out in a heat treatment furnace pre-set at heating rate of 10^0 C/min in the following sequence: (i) heating to 800^0 C and allowed to soak for 3 hours, (ii) heating to 1200^0 C and allowed to soak for 3 hours, and (iii) finally heating to 1350^0 C and allowed to soak for 3 hours. The samples were removed from the furnace and allowed to cool after which they were characterised. The picture of few of the produced ceramic composites is presented (Fig. 1).

2.4. Properties evaluation tests

2.4.1. Microstructure

The microstructure and the chemical compositions of the phases present in the test samples were examined using an ASPEX 3020 model variable pressure scanning electron microscope (SEM) equipped with Noran-Voyager energy dispersive X-ray spectroscope (EDS). The samples to be observed under the SEM were mounted on a conductive carbon imprint left by the adhesive tape prepared by placing the samples on the circular holder and coated for five minutes to enable it conduct electricity. The samples were analysed at an accelerating voltage of 15 kV for the energy dispersive X-ray spectroscopy.

2.4.2. Density

Weights of the samples in air were measured with an analytical balance and their weights in water were measured with a suspension kit and measuring cylinder at room temperature. The densities of the sintered samples were determined by Archimedes' principle based on buoyancy of water as follows:

$$\text{Density}\,(\rho) = \frac{\text{Mass (g)}}{\text{Volume (cm}^3\text{)}} \qquad (1)$$

2.4.3. Porosity

This is a physical test which shows the level at which the composites absorb solvents when placed in such environments. The weight (W_1) of the fired samples was recorded using a digital balance. The samples were then suspended in distilled water boiled to 100^0 C on a hot plate for 1 hour after which they were removed and quickly soaked in cold water for about 30 minutes and the suspended weight in cold water (W_2) was recorded. The samples were then removed from cold water gently, cleaned with a wet towel and the weight (W_3) was recorded. The apparent porosity of the samples was determined as follows:

$$P_a = \left(\frac{W_3 - W_1}{W_3 - W_2} \times 100\right)\% \qquad (2)$$

Where:
P_a = apparent porosity
W_1 = weight of fired samples
W_2 = weight in cold water
W_3 = weight in air

2.4.4. Linear shrinkage

After moulding, the length of the green (fresh) sample was measured and recorded as L_0 and the length of the fired sample L_1 was measured and recorded. The linear shrinkage was determined as follows:

$$LS = \left(\frac{L_0 - L_1}{L_0} \times 100\right)\% \qquad (3)$$

where:
LS = Linear Shrinkage

L_0 = length of the green (fresh) sample (mm)
L_1 = length of the fired sample (mm)

2.4.5. Impact energy

Impact energy test was carried out in accordance with ASTM D790 standard for which samples were prepared to size of 55 mm x 10 mm x 10 mm with a 2 mm deep V-notch at the center of the specimens. Each sample was clamped vertically with the notch facing the striker and the striker swings downwards impacting the sample at the bottom of its swing. Each sample was subjected to horizontal impact loading using an Izod impact tester under a striking pendulum velocity of 5 ms^{-1} from a height of 1.3 m. The energy absorbed to fracture each specimen was read off from the instrument's dynamometer.

2.4.6 Compressive strength

Compressive strength test was carried out on the samples having dimension 12.7 mm x 12.7 mm x 25.4 mm in accordance with ASTM D695 standard. Each of the samples was subjected to uniaxial compressive loading until the sample breaks and the strength is recorded using universal testing machine (UTM), Instron Model 3369, System No. 3369K1781, maximum speed 500 mm/min.

3. Results and discussion

3.1. Composition and phases

The XRF (Table 2) analysis of the millscale particles shows that wustite (FeO) has the highest concentration (wt. %) followed by hematite (Fe_2O_3) and magnetite (Fe_3O_4). The XRD (Fig. 2) spectra reveals that wustite (FeO), hematite (Fe_2O_3), and magnetite (Fe_3O_4) are the major mineralogical phases present in the millscale particles. The oxides exhibit characteristics peaks at various Bragg's angles where FeO peak demonstrates the highest intensity of 1500 counts at about 42°.

Iron millscale is a generic oxide consisting of FeO, Fe_2O_3 and Fe_3O_4 in differing proportions. FeO has the largest amount (69 wt. %) of the oxides in millscale and it is the closest to the equilibrium state. This implies that FeO is the most active oxide and will invariably exert profound influence on the physical and mechanical behaviours of millscale. Considering the characteristic high heat conductivity of iron (80.4 $Wm^{-1}.K^{-1}$), iron millscale as a component in a brake pad could be a potential heat dissipating material which could prevent possible adiabatic heating within the brake assembly thereby preventing heat build-up that could cause warpage of brake pad in operation which is not desirable.

SiO_2 (Table 3) is the major compound present while other compounds such as alumina (Al_2O_3), iron (iii) oxide (Fe_2O_3), magnesia (MgO), and calcium oxide (CaO) etc are in traces. The XRD spectra (Fig. 3) shows that silica sand particles exhibit characteristics peaks at various Bragg's angles. It is also observed that haematite (Fe_2O_3) and calcium oxide (CaO) peaks have broadly lower intensities compared to the silica peak. Silica sand particles exhibit characteristics peaks at various Bragg's angles with the crystalline silica peak at 26^0 having the highest intensity (700 counts) followed by alumina (Al_2O_3) with intensity of 160 counts. As established by [10], silica is the major mineralogical phase in the diffraction spectra while other compounds have broadly lower intensities.

Silica is a chemically inert and hard material with low density, 2.65 g/cm³ and high melting point (1610^0 C). These characteristics can be attributed to the strength of the bonds between the atoms. Further, its low permeability to liquid ingression has the potential for improved dimensional stability due to its low moisture absorption behaviour coupled with lighter weight arising from low density. The XRF result (Table 3) indicates the presence of up

to 0.2 % alumina in the silica. This represents a significant difference from the common available silica sand. The suitability of silica as brake pad material is complimented by its availability thereby making it cost competitive.

MgO (Table 4) is the dominant compound present with up to 98.8 wt. %. This level of purity is capable of enhancing the material's intrinsic physical and mechanical properties. The XRD spectra (Fig. 4) confirms magnesia (MgO) as the major mineralogical phase with the highest peak of 4500 counts at almost 27° whereas the minor phase, calcium oxide (CaO) has a peak of 500 counts at Bragg's angles 37° and 43°. Magnesia has a high melting temperature of 2827 ± 30^0 C, specific heat capacity of 37.8 $Jmol^{-1}$. K^{-1} and has been proven to be thermally stable at elevated temperatures [11]. The material also combines these characteristics with excellent abrasion and erosion resistance [12]. Thus, magnesia is a potential suitable friction/thermal matrix material for application in areas where high resistance to thermal stress and abrasive wear are required
The chemical composition (Table 5) of the as-received bentonite powder by XRF shows that SiO_2 (63 wt. %) and Al_2O_3 (23 wt. %). The XRD spectra (Fig. 5) shows that SiO_2 has the highest intensity among the compounds. These results indicate that the bentonite used belongs to the alumino-silicate group. It has been established that bentonite possesses high thermal shock resistance, refractoriness, high compressive strength, resistance to abrasive wear, and low porosity that are desirable [13]. It also has the potential to confer cohesion and strength on silica sand [14].

3.2. Chemical reactions

Iron (II) oxide (FeO) particles react with water to form iron (II) hydroxide which decomposes at high sintering temperature.

$FeO\ (s) + H_2O\ (s) \longrightarrow Fe(OH)_2$ .....(4)

$Fe(OH)_2 \longrightarrow FeO(s) + (H_2O$ evaporation)..... (5)

Magnesia (MgO) has high affinity for water. Hence, reacts also with water to form Magnesium hydroxide which also decomposes at high sintering temperature.

$MgO\ (s) + H_2O\ (l) \longrightarrow Mg(OH)_2$ .....(6)

$Mg(OH)_2 \longrightarrow MgO(s)+(H_2O$ evaporation)..... (7)

Silica reacts with bentonite in the presence of water during high temperature sintering to form a ceramic compound (mullite) which exhibits excellent high temperature properties with improved thermal shock and thermal stress resistance owing to the low thermal expansion, good strength, and high wear resistance.

$SiO_2\ (s) + SiO_2{\cdot}Al_2O_3\ (s) + H_2O \longrightarrow 3SiO_2.2Al_2O_3$ (mullite) (s) + (H_2O evaporation)..... (8). In all these reactions, there is evaporation of water from the products of reaction due to the high sintering temperature (800-1350^0 C) used leaving FeO, MgO, and mullite as constituents of the samples.

3.3. Microstructure

The SEM micrographs (Figs. 6a – 8a) show that the samples are made up of different additives which confirm that they are heterogeneous with differences in the geometry of the particles which are globular and needle-like. The EDS spectrographs show a good combination of the elemental distribution which also reflects on the heterogeneous nature of the composites. Different sizes of particles or elements also contributed to the heterogeneous distribution. The EDS spectrographs of the composites show the presence of O, Si, Al, Mg, Fe, and Ca but the unreinforced (control) does not contain Fe (Fig. 6b). There are also indistinguishable peaks in the spectrographs indicating the presence of other elements in very small amount. The white spots in the micrographs are particles of the magnesia while the dark spots are FeO particles from the millscale. The ash coloured needle-like region of the matrix indicates the presence of mullite ($3Al_2O_3{\bullet}2SiO_2$), a highly crystalline

compound from bentonite clay-silica mixture (Figs 6a – 8a) formed due to the high sintering temperature (1350^0 C) used in the production of the samples. Generally, from the micrographs of the reinforced samples (Figs. 7a, 8a), the iron millscale (FeO) particles are seen to be well distributed in the matrix without any form of segregation. The interfacial bonding between the reinforcement and the matrix is enhanced by the relatively close-spacing of the FeO particles. This also suggests a good vitrification of the reinforced composites during sintering

3.4. Density

The unreinforced hybrid ceramic composite has a density of 2.35 g/cm^3 while the reinforced composite at 30 wt. % has a density of 3.05 g/cm^3 which represents 29.79 % increase in density. There is a progressive increase in the densities of the reinforced hybrid ceramic composites with increasing weight fraction of the millscale particles (Fig. 9). This may be attributed to a relatively high packing factor of millscale particles as its concentration increases within the matrix thereby increasing the density of the composites. This behaviour is further enhanced by the effective fusion of millscale particles during sintering to form a coherent body with the matrix. This suggests a good vitrification of the reinforced composites during sintering. This agrees well with the fact that iron based friction materials retain some particular properties such as high density level [15]. The density increment is also seemed to be due to deposition of iron as a result of diffusion into the ceramic phase which agrees well with the result of iron infiltration in ceramics as reported during In-situ TiC-Fe-Al_2O_3-TiAl/Ti_3Al composite coating processing using centrifugal assisted combustion synthesis [16].

3.5. Porosity

The porosity level of the unreinforced hybrid ceramic composite is 1.57 % which progressively decreased to 1.24 % at 30 wt. % for the 106 µm reinforced composite (Fig. 10) with percentage decrease of 21 % which is quite significant. This compares very well with conventional or commercial brake pads. The decrease in the values of porosity with increasing weight fraction of millscale particles is due to particle agglomeration which suggests an improved vitrification of the reinforced composites during high temperature sintering. Low porosity enhances the achievement of compact and dense composite materials with the tendency to improve the mechanical properties [17]. This is also in agreement with the postulation that pores tend to shrink during sintering resulting in good bonding of the particles which greatly reduces porosity and enhances plasticity of ceramic composites reinforced by metal particles [18].

3.6. Linear shrinkage

The linear shrinkage level of the unreinforced hybrid ceramic composite is 1.59 % which progressively decreased to 1.39 % at 30 wt. % reinforcement for the 106 µm reinforced composite (Fig. 11). The percentage decrease (13 %) is quite significant. This could be as a result of the bonding between particles at high sintering temperature. This agrees well with the postulation that good bonding of particles during high sintering temperature greatly enhances the linear shrinkage of composites with reduction in inter-particles separation [19].

3.7. Impact energy

The impact energy gives an indication of the toughness of the composite and it increases progressively with increase in reinforcement. The maximum impact energy (43.07 J) was obtained by sample A at 25 wt. % (Fig. 12) representing a substantial 53 % increase over the unreinforced. The significant increase in impact energy is strongly predicated on fine particles size,

their uniform distribution within the matrix, and the strong interfacial bonding between the metallic and the ceramic phases [20]. The increase in the weight fraction of FeO particles (metal phase) confers on the samples the level of plasticity sufficient to absorb energy, thereby increasing the impact energy. Invariably, increasing the weight fraction of iron millscale particles (FeO) led to increase in elasticity within the composite core thereby increasing its toughness [21].

3.8. Compressive strength

The compressive strength of a material is the measure of its capacity to withstand loads tending to cause lateral reduction. As evident from Fig. 13, there is an increase in the compressive strength of all the samples with the 106 µm millscale reinforced exhibiting the maximum compressive strength (114.17 MN/m^2) at 25 wt. % representing 42 % increase over the unreinforced. Small particles enhance densification which correspondingly improves the mechanical properties [20]. Small particles are more effective in strengthening composites than coarse particles of the same weight fraction because smaller grain sizes increase the frequency with which dislocations encounter grain boundaries, thus requiring larger stresses for deformation to occur [22]. The strong interfacial bonding between the metallic and the ceramic phases also contributed to the enhancement of the compressive strength.

Further comparison with the results of previous works on existing conventional or commercial brake pads (Table 6) shows that the compressive strength of the composite compares very well with other brake pads. This is an indication that it will perform well in service.

4. Conclusion

The development and charaterisation of iron millscale particles reinforced ceramic matrix composite using varied weight percentages of reinforcement has been undertaken with the 106 µm millscale reinforced exhibiting desirable physical and mechanical properties in terms of density (2.97 g/cm^3), porosity (1.24 %), linear shrinkage (1.39 %), impact energy (43.07 J), compressive strength (114.17 MN/m^2), and shear strength (63.86 MN/m^2). The low density implies low weight which will result into low fuel consumption for aircrafts and automobiles. The low porosity obtained enhances the achievement of compact and dense composite brake pad materials with the tendency to improve the mechanical properties while relatively low linear shrinkage will ensure dimensional stability under service conditions. These values compare very well with the values of brake pads obtained in previous works and conventional/commercial brake pads (Table 6) indicating a potential for effective performance in service.

References

[1] S.N. Nagesh, C. Siddaraju, S.V. Prakash, M.R. Ramesh, Characterisation of brake pads by variation in composition of friction materials, Elsevier, Proceedia Materials Science, 5 (2014) 295-302.

[2] J. Aderiye, Kaolin mineral material for automobile ceramic brake pad manufacturing industry, International Journal of Technology Enhancements and Emerging Engineering Research, 2 3 (2014) 84-88.

[3] R.O. Edokpia, V.S. Aigbodion, O.B. Obiorah, C.U. Atuanya, Evaluation of the properties of eco-friendly brake pad using egg shell particles–gum arabic. ScienceDirectR, Elsevier B.V. (2014), DOI: 10.1016/j.rinp.2014.06.003.

[4] T.K. Fabemigun, O.D. Fagbemi, O. Otitoju, E. Mgbachiuzor, C.C. Igwe, Pulp and paper-making potential of corn husk, International Journal of AgriScience, 4 4 (2014) 209- 213.

[5] A.A. Adebisi, M. Maleque, Q.H. Shah, Surface temperature distribution in a composite brake rotor, International Journal of Mechanical and Materials Engineering, 6 3 (2011) 356- 361.

[6] P. Mahale, A. Bohari, M.P. Raajha, 2014. Effect of thermal behaviour of friction man-made wonder, Golden jubilee commemoration lecture (tenth in the series), Foundry & Forge & Aerospace Divisions, Hindustan Aeronautics Limited, Bangalore, The Indian Institute of Metals, Bangalore Chapter, (2014) 1-70, Technical Papers, DOI: 10.4271/2014-01-2514.

[7] M. Nanko, High-temperature oxidation of ceramic matrix composites dispersed with metallic particles. Sci Technol Adv Mater, 6 (2005) 129–134.

[8] J.Q. Li, X.R. Zeng, J.N. Tang, P. Xiao fabrication and thermal properties of ysz-nicr joint with an interlayer of ysz-nicr functionally graded materials, J Eur. Ceram. Soc., 23 (2003) 1847–1853.

[9] B. Kieback, A. Neubrand, H. Riedel Processing techniques for functionally graded materials, Mater. Sci. Eng., A362 (2003) 81–105.

[10] A.O. Ajayi, A.Y. Atta, B.O. Aderemi, S.S. Adefila, Novel method of metakaolin de-alumination-preliminary investigation, Journal of Applied Sciences Research, 6 10 (2010) 1539-1546.

[11] www.rse.org/chemistryworld/2014 (accessed 9.4.16).

[12] M.A. Aramendia, V. Borau, C. Jimenez, J.M. Marinas, J.R. Ruiz, F.J. Urbano, Applied Catalysis, 244 2 (2003) 207-215.

[13] M.S. Abolarin, O.A. Olugboji, I.C. Ugwoke. Determination of moulding properties of locally available clays for casting operations. AU Journal of Technology, 9 4 (2006) 238-242.

[14] P.O. Atanda, O.E. Olorunniwo, K. Alonge, O.O. Oluwole. Comparison of bentonite and cassava starch on the moulding properties of silica sand. International Journal of Materials and Chemistry 2 4 (2012) 132-136, DOI: 10.5923/j.ijmc.20120204.03.

[15] M. Asif, K. Chandra, P.S. Misra, Development of iron based brake friction materials by hot preform forging technique used for medium to heavy duty applications, Journal of Minerals and Materials Characterisation and Engineering, 10 3 (2011) 231-244.

[16] R. Mahmoodian, M.A. Hassan, M. Hamdi, R. Yahya, R.G. Rahbari, In-situ TiC-Fe-Al_2O_3-TiAl/Ti_3Al composite coating processing using centrifugal assisted combustion synthesis, Composites Part B: Engineering 59 (2014) 279-284.

[17] C.M. Ruzaidi, H. Kamarudin, J.B. Shamsul, M.M.A. Abdullah, Mechanical Properties and Wear Behavior of Brake Pads Produced from Palm Slag, Advanced Materials, 341-342 (2012) 26-30.

[18] V.S. Aigbodion, J.O. Agunsoye, V. Kalu, F. Asuke, S. Ola, Microstructure and mechanical properties of ceramic composites, Journal of Minerals & Materials Characterization & Engineering, 9 6 (2010) 527-538.

[19] C.I. Nwoye, E.O. Obidiegwu, N.E. Nwankwo, Model for computational analysis and predictive assessment of bulk density of fired bricks based on incurred shrinkage, Journal of Innovative Research in Engineering and Science, 2 (2011) 74-82.

[20] M.S. Randelovic, A.R. Zarubica, M.M. Purenovic, New composite materials in the technology for drinking water purification from ionic and colloidal pollutants, 2012, http://dx.doi.org/10.5772/48390 (accessed 20. 10. 2015).

[21] R. Kaundal, A. Patnaik, A. Satapathy, Solid particle erosion of short glass

fiber reinforced polyester composite, American Journal of Materials Science, 2 2 (2012) 22-27.

[22] H. Lee, R.F. Speyer, Hardness and fracture toughness of pressureless sintered boron carbide (B_4C), Journal of American Ceramic Society, 85 5 (2002) 1291–1293.

[23] U.D. Idris, V.S. Aigbodion, I.J. Abubakar, C.I. Nwoye, Eco-friendly asbestos free brake-pad: using banana peels, Journal of King Saud University-Engineering Sciences, 27 2 (2015) 185–192.

[24] N.A. Ademoh, A.I. Olabisi, Development and evaluation of maize husks (asbestos-free) based brake pad, Industrial Engineering Letters, 5 2 (2015) 67-80.

FIGURES

Fig. 1. Picture of the produced hybrid ceramic composite.

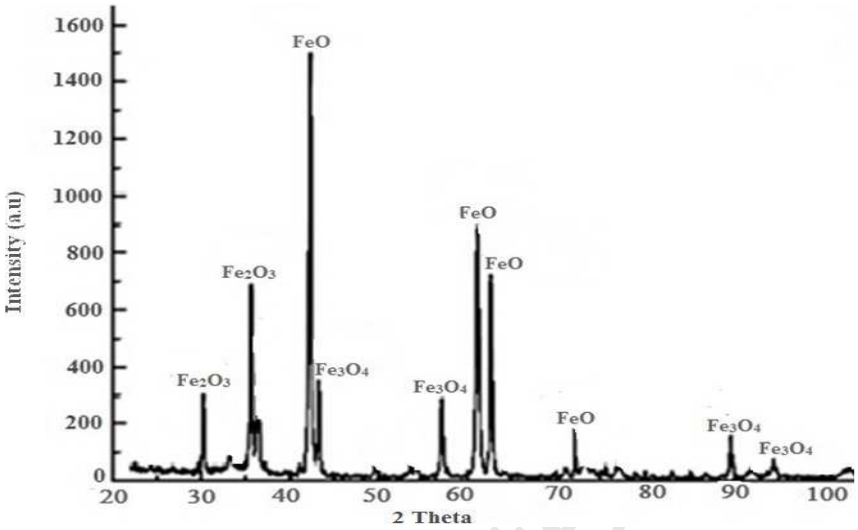

Fig. 2. XRD spectra of iron millscale.

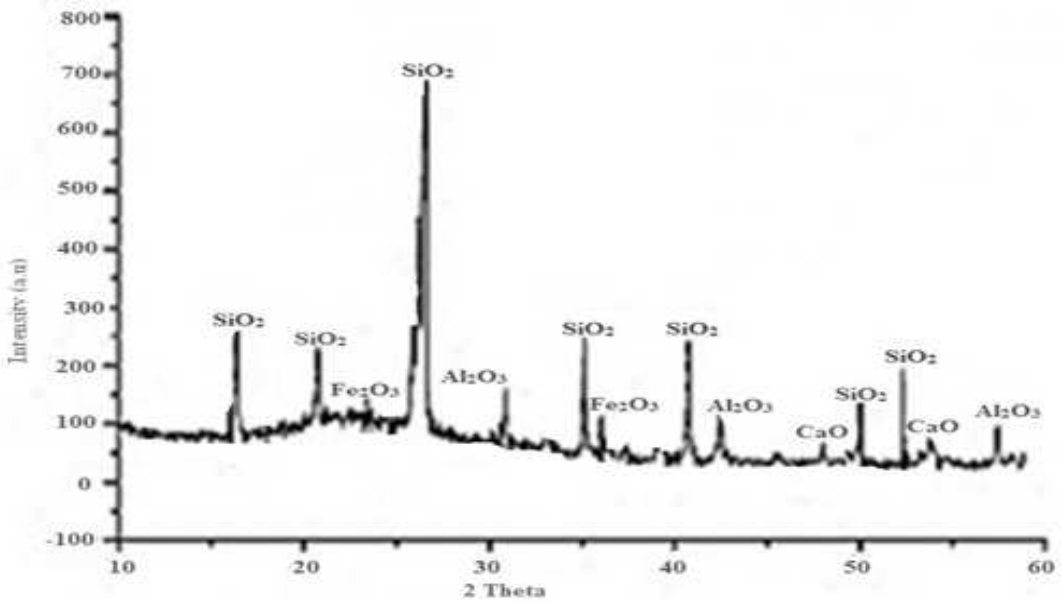

Fig. 3. XRD spectra of silica sand particles.

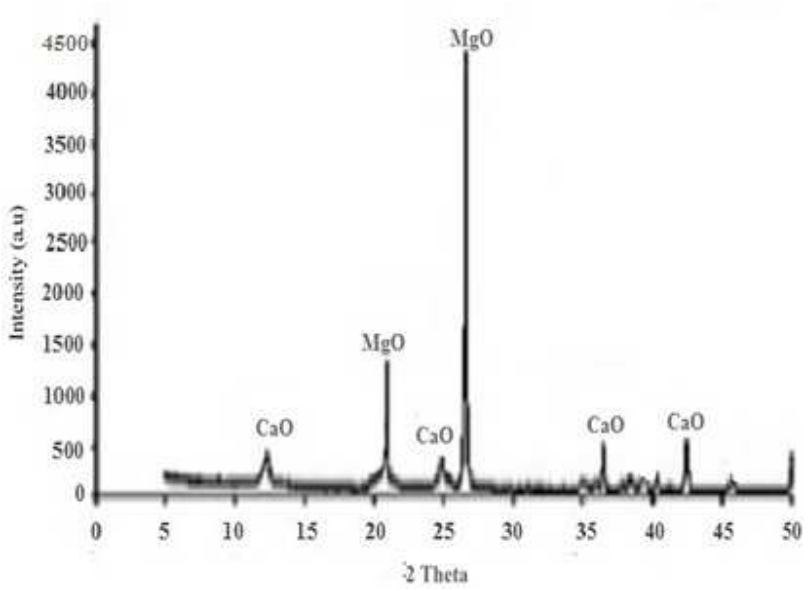

Fig. 4. XRD spectra of magnesia powder.

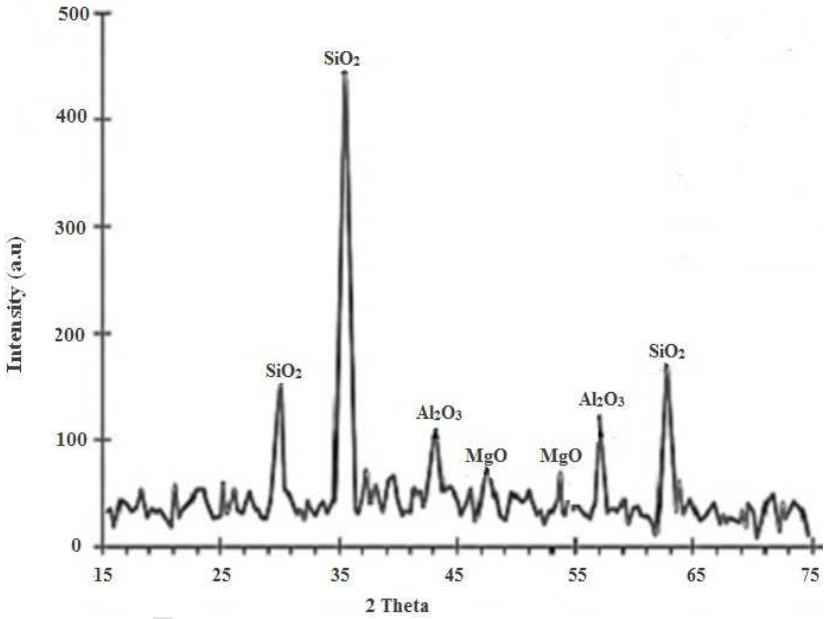

Fig. 5. XRD spectra of the as-received bentonite clay powder.

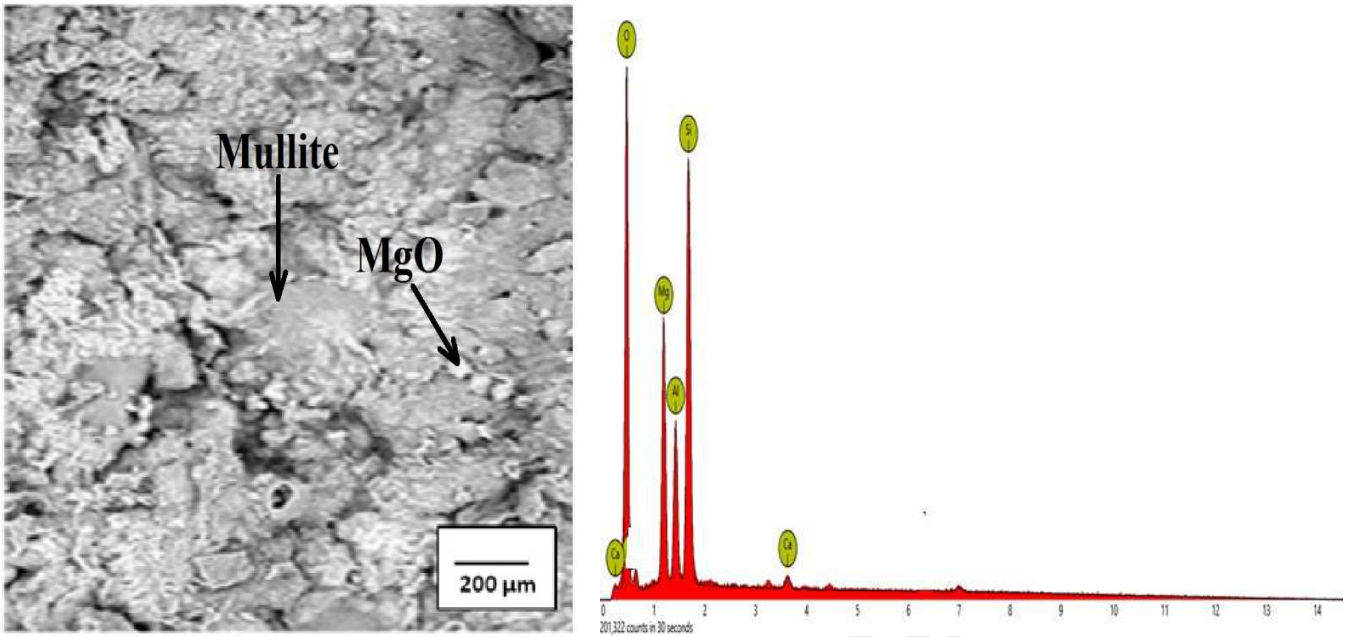

(a) (b)

Fig. 6. (a) SEM (b) EDS of the unreinforced ceramic composite (control).

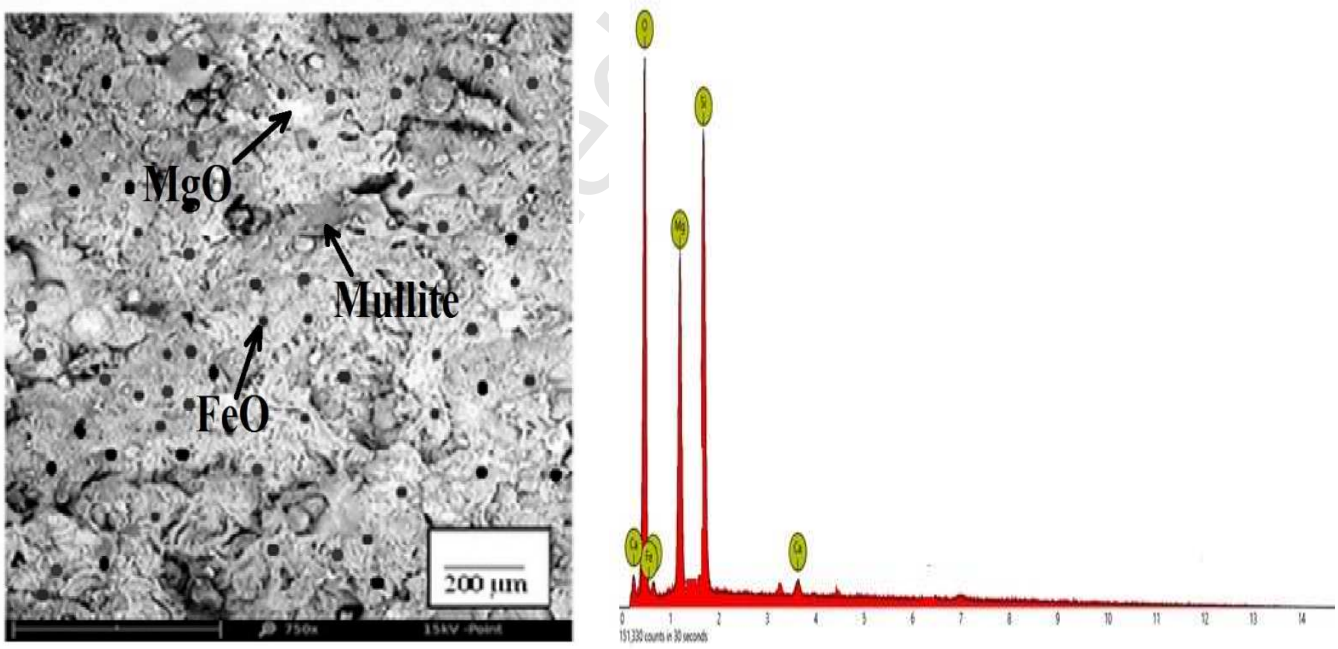

(a) (b)

Fig. 7. (a) SEM (b) EDS of the 10 wt. % 106 µm millscale reinforced ceramic composite.

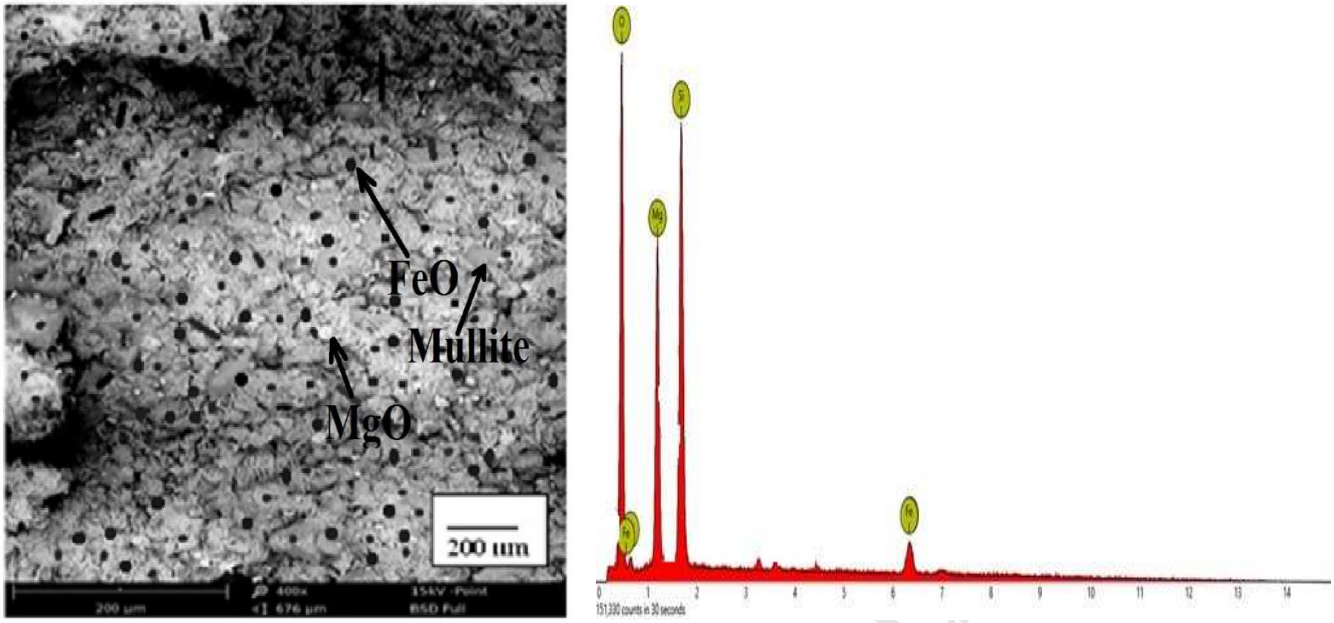

(a) (b)

Fig. 8. (a) SEM (b) EDS of the 25 wt. % 106 µm millscale reinforced ceramic composite.

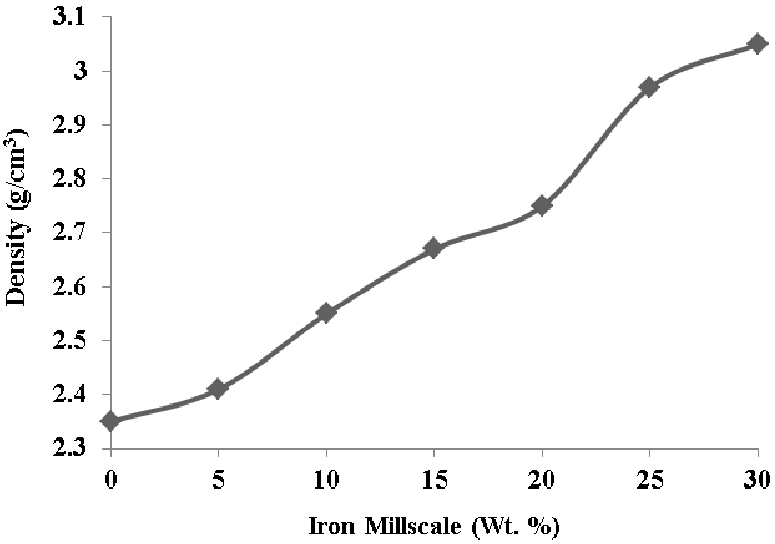

Fig. 9. Effect of varied iron millscale particles addition on the density of 106 µm millscale particles reinforced ceramic composites.

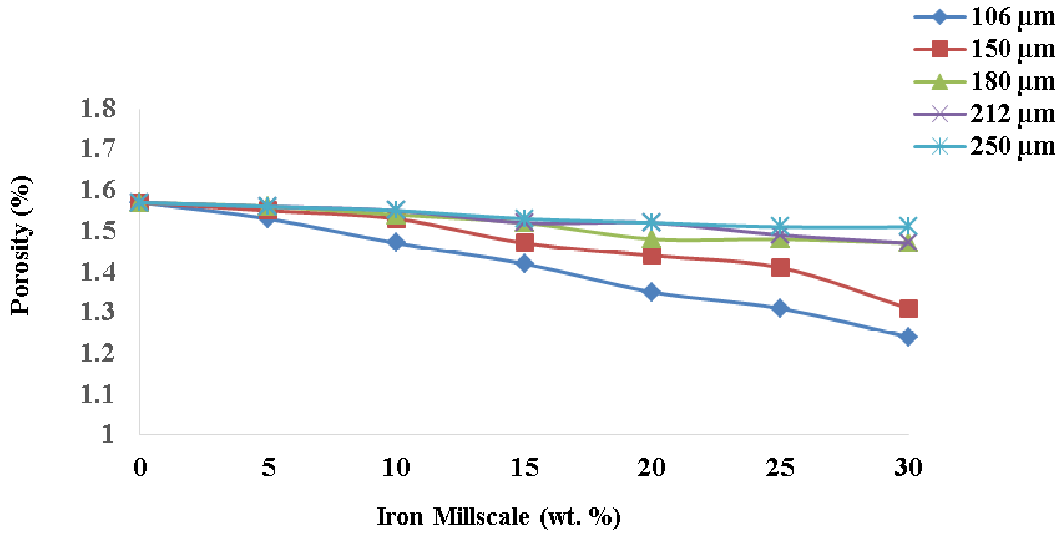

Fig. 10. Effect of varied iron millscale particles addition on porosity of the composites.

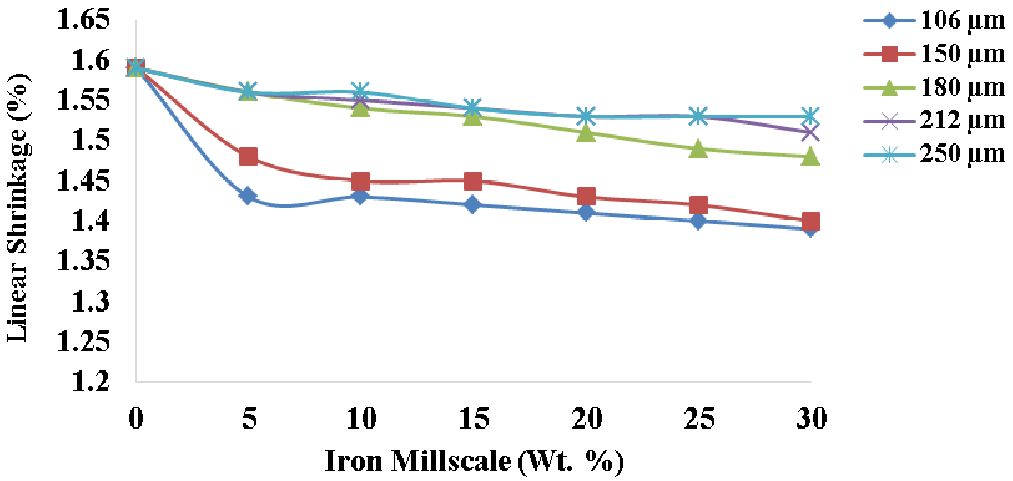

Fig. 11. Effect of varied iron millscale particles addition on linear shrinkage of the composites.

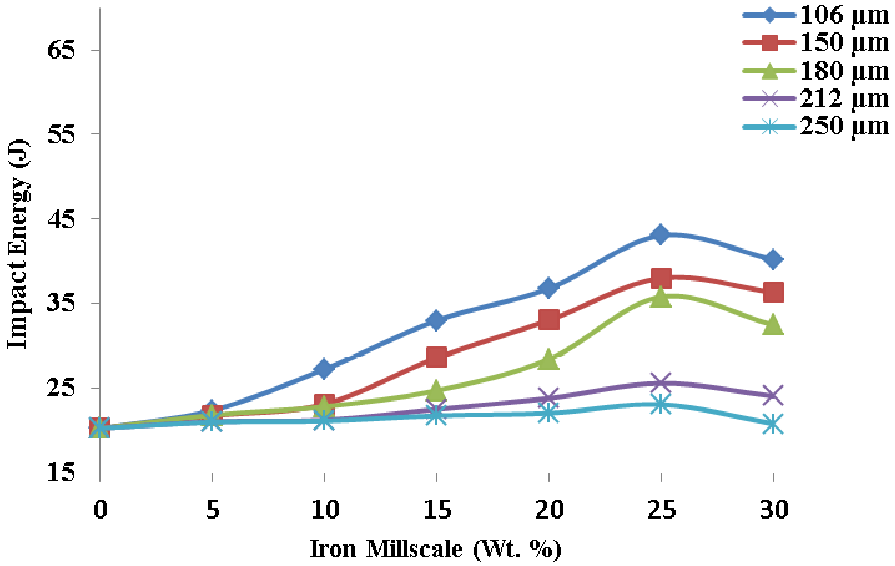

Fig. 12. Effect of varied iron millscale particles addition on impact energy of the composites.

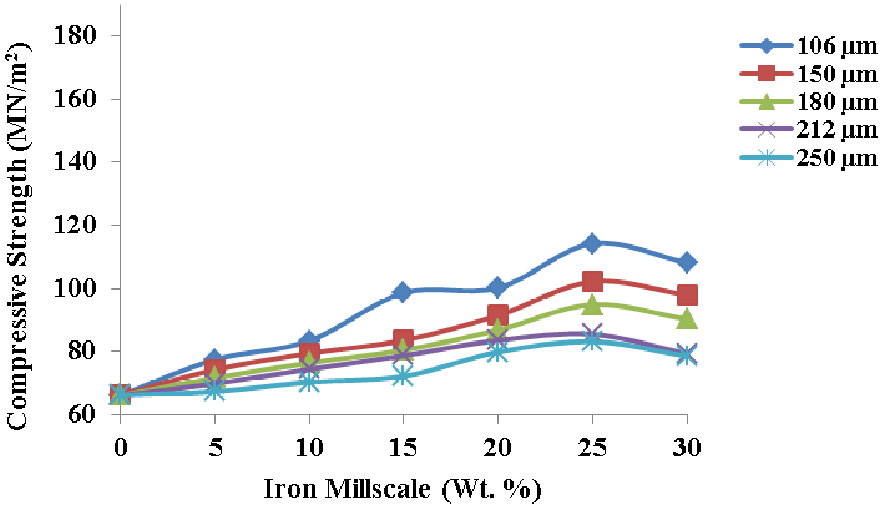

Fig. 13. Effect of varied iron millscale particles addition on compressive strength of the composites.

TABLES

Table 1
Materials formulation

Reinforcement		Matrix blend	
Weight (%)	Weight (g)	Weight (%)	Weight (g)
0 (Control)	0	100	80
5	4	95	76
10	8	90	72
15	12	85	68
20	16	80	64
25	20	75	60
30	24	70	56

Table 2
Chemical composition of iron millscale by XRF

Compounds	FeO	Fe_2O_3	Fe_3O_4	SiO_2	MgO	CaO	MnO	L.O.I
Weight (%)	68.809	24.735	6.184	0.011	0.016	0.220	0.024	0.001

Table 3
Chemical composition of silica sand by XRF

Compounds	SiO_2	Al_2O_3	Fe_2O_3	FeO	CaO	MnO	MgO	Na_2O	K_2O	M.O.I	L.O.I.
Wt. %	98.988	0.180	0.152	0.024	0.016	0.009	0.024	0.003	0.002	0.001	0.491

Table 4
Chemical composition of magnesia by XRF

Components	MgO	CaO	SiO_2	M.O.I	L.O.I
Wt. %	98.840	0.025	0.007	0.001	0.012

Table 5
Chemical composition of as-received bentonite powder by XRF

Compounds	SiO_2	Al_2O_3	MgO	Fe_2O_3	CaO	Na_2O	K_2O	TiO_2	L.O.I
Wt. %	62.986	23.247	3.864	2.673	1.316	2.457	0.524	0.136	2.797

L.O.I = Loss on Ignition
M.O.I = Moisture

Table 6
Comparison with other brake pads [23, 24]

Authors/Study	Density (g/cm^3)	Linear Shrinkage (%)	Porosity (%)	HDN	CS (MPa)	SS (MPa)
Bagasse based brake pad	1.43	-	3.48	100.5 MPa	105.6	-
Uncarbonized banana peels based brake pad	1.26	-	3.21	98.8 BHN	95.6	-
Carbonized banana peels based brake pad	1.2	-	3.0	71.6 BHN	61.2	-
PKS+CS+MH (300 µm) based brake pad	0.853	-	0.91	127.8 MPa	10.3	-
Commercial asbestos based brake pad	1.89	-	0.9	101 MPa	110	54.6

PKS = Palm kernel shell
CS = Coconut shell
MH = Maize husk
HDN = Hardness
CS = Compressive strength
SS = Shear strength
BHN = Brinell hardness number

Development and Characterisation of iron millscale particles reinforced ceramic matrix composite

Stephen I. Durowaye [a,] , Olatunde I. Sekunowo [a], Abdulganiyu I. Lawal [a], Olusola E. Ojo [b]

[a] *Department of Metallurgical and Materials Engineering, University of Lagos, Akoka, Lagos, Nigeria*
[b] *Federal Institute of Industrial Research (FIIRO), Oshodi, Lagos, Nigeria*

** Corresponding author. Tel.: +234 8036844029.*
E-mail address: durosteve02@yahoo.com (S.I. Durowaye).

Authors' Details

Stephen I. Durowaye (Ph.D)

Durowaye is a metallurgical & materials engineer with 12 years of industrial experience. He is presently a lecturer in the Department of Metallurgical & Materials Engineering, University of Lagos, Nigeria. He is actively involved in teaching and research. He is a corporate member of the Nigerian Society of Engineers (MNSE). He has 20 research publications in international journals.

Olatunde I. Sekunowo (Ph.D)

Sekunowo is a seasoned metallurgical & materials engineer whose work-experience in the steel industry spanned sixteen years. In 2006, he joined the academic staff of the department of Metallurgical & Materials Engineering, University of Lagos, Nigeria where he has been actively involved in teaching and research. He is a senior lecturer. His research focus is mainly in the areas of developing innovative materials processing methods, characterisation and waste recycling (Value-addition engineering). He holds a Ph.D (Mechanical Metallurgy), a COREN (Council for the Regulation of Engineering practice in Nigeria) registered engineer and a corporate member of Nigerian Society of Engineers. He has over 40 research publications in international journals.

Abdulganiyu I. Lawal (Ph.D)

Lawal is a Professor of metallurgical & materials engineering in the Department of Metallurgical & Materials Engineering, University of Lagos, Nigeria. He has over 20 years of teaching and research experience. He is a member of the Nigerian Society of Engineers (MNSE) and other professional bodies. He has over 50 research publications in international journals.

Olusola E. Ojo (B.Sc, M.Sc)

Ojo is a metallurgical & materials engineer with 20 years of industrial experience. He is a corporate member of the Nigerian Society of Engineers (MNSE). He has 10 research publications in international journals.